Articles in PresS. Am J Physiol Endocrinol Metab (July 1, 2014). doi:10.1152/ajpendo.00187.2014

Lipid storage by adipose tissue macrophages regulates systemic glucose tolerance

Myriam Aouadi[1], Pranitha Vangala[1], Joseph C. Yawe[1], Michaela Tencerova[1], Sarah M. Nicoloro[1], Jessica L. Cohen[1], Yuefei Shen[1], and Michael P. Czech[1,*].

AUTHOR CONTRIBUTIONS

M.A. and M.P.C. conceptualized, designed the study and wrote the manuscript P.V., J.C.Y., S.M.N., M.T., J.L.C., Y.S., performed experiments, and all authors participated in designing experiments, and analyzing and interpreting data.

[1]Program in Molecular Medicine, University of Massachusetts Medical School, Worcester, Massachusetts 01605, USA.

Running head: Lipid storage within adipose tissue macrophages

Corresponding author:
Michael P. Czech
Program in Molecular Medicine
373 Plantation Street, Suite 100
University of Massachusetts Medical School
Worcester, MA 01605
Tel. 1 508 856 2254
Fax. 1 508 856 1617
Michael.Czech@umassmed.edu

Please address scientific correspondence to:
Michael.Czech@umassmed.edu or Myriam.Aouadi@umassmed.edu

ABSTRACT

Pro-inflammatory pathways in adipose tissue macrophages (ATMs) can impair glucose tolerance in obesity, but ATMs may also be beneficial as repositories for excess lipid that adipocytes are unable to store. To test this hypothesis, we selectively targeted visceral ATMs in obese mice with siRNA against lipoprotein lipase (LPL), leaving macrophages within other organs unaffected. Selective silencing of ATM LPL decreased foam cell formation in visceral adipose tissue of obese mice, consistent with a reduced supply of fatty acids from VLDL hydrolysis. Unexpectedly, silencing LPL also decreased the expression of genes involved in fatty acid uptake (CD36) and esterification in ATMs. This deficit in fatty acid uptake capacity was associated with increased circulating serum free fatty acids (FFAs). Importantly, ATM LPL silencing also caused a marked increase in circulating fatty acid binding protein 4 (fabp4/aP2), an adipocyte-derived lipid chaperon previously reported to induce liver insulin resistance and glucose intolerance. Consistent with this concept, obese mice with LPL-depleted ATMs exhibited higher hepatic glucose production from pyruvate and glucose intolerance. Silencing CD36 in ATM also promoted glucose intolerance. Taken together, the data indicate that LPL secreted by ATMs enhances their ability to sequester excess lipid in obese mice, promoting systemic glucose tolerance.

Keywords: siRNA, adipose tissue macrophages, obesity, insulin resistance, foam cells.

INTRODUCTION

The inability to appropriately expand adipose tissue (AT) in human obesity may lead to ectopic lipid deposition in liver and skeletal muscle, and may be an underlying cause of insulin resistance (14, 17, 26). Accumulation of immune cells including macrophages in the visceral AT of obese mice and humans creates a chronic inflammatory state that correlates with insulin resistance (18, 23, 30). These ATMs secrete cytokines and other factors that may impair adipocyte capacity to store lipids (18, 23, 30), promoting the ectopic deposition of lipid in non-adipose tissues. However, some data indicate a beneficial role of ATMs, for example, in increasing adipose lipid storage (16). ATMs are also required for maintenance of AT homeostasis by regulating angiogenesis, extracellular matrix remodeling, and clearance of dead cells in AT (7, 11, 15, 24, 27). It is therefore likely that macrophages exert multiple, even opposing effects on adipocytes, depending upon physiological conditions.

In order to determine if ATMs contribute to lipid storage and glucose tolerance, we silenced the expression of lipoprotein lipase (LPL) by ATMs. LPL is released by cells within AT and is translocated to the lumen of adipose capillaries, where it binds the glycosylphosphatidylinositol-anchored high-density lipoprotein-binding protein 1 (GPIHBP1) (1, 21). LPL is known to control localized VLDL triglyceride hydrolysis and uptake of fatty acids into the tissue (1, 21). The contribution of macrophage-LPL in this function is suggested by experiments showing that depletion of macrophage LPL is effective in reducing lipid laden foam cell formation in arteries of LDL receptor null mice (5). Here we employed glucan encapsulated siRNA particles (GeRPs) to silence gene expression of LPL specifically in ATMs in obese mice without perturbing macrophages in other tissues, including liver (2, 3, 29). Such selective silencing of LPL in ATMs of obese mice, decreased foam cell formation in AT and caused a marked impairment in glucose tolerance, indicating ATMs contribute to beneficial lipid storage within AT.

METHODS

All procedures involving animals were approved by the Institutional Animal Care and Use Committee at the University of Massachusetts Medical School.

Preparation of Glucan Encapsulated siRNA Particles (GeRPs)

To load siRNA in glucan shells, 3 nmoles siRNA (Dharmacon) was incubated with 50 nmoles Endo-Porter (Gene Tools) in 30 mM sodium acetate pH 4.8 for 15 min at RT in a final volume of 20 µl. The siRNA/Endo-Porter solution was added to 1 mg ($\approx 10^9$) of glucan shells and then vortexed and incubated for 1 hour. The siRNA loaded GeRPs were then resuspended in PBS and sonicated to ensure homogeneity of the GeRP preparation. GeRPs were kept at 4°C.

Peritoneal macrophage preparation

Eight-week old C57BL6/J male mice were ip injected with 4% thioglycollate broth (Sigma-Aldrich). Five days following injection, the peritoneal cavity was washed with PBS and peritoneal fluid was filtered through a 70 µm diameter pore nylon mesh and centrifuged. The pellet was first treated with red blood cell lysis buffer and plated in DMEM supplemented with 10% fetal bovine serum (FBS), 50 µg/ml streptomycin and 50 units/ml penicillin. 24 hours after isolation, the PECs (peritoneal exudate cells) were treated with siRNA.

Gene silencing by siRNA/EP particles *in vitro* in cell culture

160 pmoles siRNA (Dharmacon) was incubated with 3 nmoles EP in PBS for 15 min and added to $1x10^6$ cells. 48 hours after treatment mRNA, media or protein were harvested.

GeRP administration and tissue isolation

Eight week-old C57BL6/J or five week-old *ob/ob* male mice were ip injected once a day for five days with 5.6 mg/kg GeRPs loaded with 2.1 mg/kg EP and 0.262 mg/kg siRNA. Further analyses were performed 24 hours after the last injection. siRNA containing GeRPs are taken up by phagocytic cells such as dendritic cells, macrophages and neutrophils.

Isolation of adipocytes, stromal vascular fraction (SVF) and ATMs.

Epididymal fat pads were mechanically dissociated using the gentleMACS Dissociator (Miltenyi Biotec) and collagenase digested at 37°C for 45 minutes, in Hank's buffered saline solution (HBSS) (Gibco, Life technologies), containing 2% bovine serum albumin (American Bioanalytical) and 2 mg/ml collagenase (Sigma-Aldrich). Samples were then filtered through 100 μm diameter pore nylon mesh and centrifuged. The adipocyte layer was collected and washed for further analysis. The pelleted cells were collected as the SVF. The SVF cells were then treated with red blood cell lysis buffer and washed in PBS and plated or directly harvested for further analysis. For ATM isolation, the SVF pellet was resuspended in 1 mL selection buffer (PBS, 2 mmol/L EDTA, and 0.5% BSA), and the CD11b-positive cells were selected using CD11b microbeads (Miltenyi Biotec), according to the manufacturer's instructions.

Isolation of RNA and Real Time PCR

RNA isolation was performed according to the Trizol Reagent Protocol (Invitrogen). cDNA was synthesized from 0.5-1 μg of total RNA using iScript cDNA Synthesis Kit (Bio-Rad) according to the manufacturer's instructions. For real time PCR, synthesized cDNA, forward and reverse primers along with the iQ SYBR Green Supermix were run on the CFX96 Realtime PCR System (Bio-Rad). The ribosomal mRNA, 36B4 was used as an internal loading control, as its expression did not change over a 24 h period with the addition of LPS or siRNA against the genes used in this study.

Western-Blot

Protein samples were separated on a 12% SDS-polyacrylamide gel and transferred to a nitrocellulose membrane. Membranes were then analyzed by Western blot analysis using anti-LPL (Abcam) and anti-actin (Sigma-Aldrich) antibodies.

Flow cytometry

SVF cells from mice treated with FITC-GeRPs were incubated for 20 min in blocking buffer containing 1% BSA and Fc block (eBioscience) for 15 minutes at 4°C to block non-specific binding. Cells were then counted and incubated for an additional 20 minutes

in the dark at 4°C with fluorophore-conjugated primary antibodies or isotype control antibodies (AbD Serotec). Antibodies used in these studies included: F4/80-APC (AbD Serotec), CD11b-PerCP-Cy5.5 (BD bioscience) and Bodipy-FITC (Invitrogen).
Subsequently cells were analyzed by flow cytometry in a LSRII cytometer (BD Bioscience). FlowJo software (Treestar) was used to identify the different cell populations. 100,000 events were recorded.
For sorting experiments, SVF cells were run through a FACS Vantage (BD Bioscience). Both FITC+ and FITC- populations were collected and RNA was harvested for RT-PCR.

Microscopy

For SVF, fixed cells were incubated with rat anti-mouse F4/80 primary antibody (AbD-Serotec) followed by goat anti-rat Alexa fluor 594 secondary antibody (Invitrogen). Cells were mounted in Prolong Gold anti-fade with DAPI (Invitrogen).
Cell images were obtained with a Solamere CSU10 Spinning Disk confocal system mounted on a Nikon TE2000-E2 inverted microscope.
For tissues, fixed sections were H&E stained. Images were obtained using a Zeiss Axiovert 200 inverted microscope equipped with a Zeiss AxioCam HR CCD camera with 1,300 × 1,030 pixels basic resolution and a Zeiss Plan NeoFluar 20×/0.50 Ph2 (DIC II) objective.

Transmission electron microscopy

Samples were processed and analyzed at the University of Massachusetts Medical School Electron Microscopy core facility according to standard procedures. Briefly, pieces of whole adipose tissue were fixed in 2.5% gluteraldehyde in 0.1 M Sodium Cacodylate buffer and left overnight at 4^{o}C. The samples were then rinsed twice in the same fixation buffer and post-fixed with 1% osmium tetroxide for 1h at room temperature. Samples were then washed twice with DH_2O for 5 minutes and then dehydrated through a graded ethanol series of 20% increments, before two changes in 100% ethanol. Samples were then infiltrated first with two changes of 100% Propylene Oxide and then with a 50%/50% propylene oxide / SPI-Pon 812 resin mixture. The following day, three changes of fresh 100% SPI-Pon 812 resin were done before the samples were

polymerized at 68^{o}C in plastic capsules. The samples were then thin sectioned and the sections were placed on copper support grids, and contrasted with Lead citrate and Uranyl acetate. Sections were examined using the FEI Tecani 12 BT with 80Kv accelerating voltage, and images were captured using a Gatan TEM CCD camera.

TG, LDL/VLDL, HDL cholesterol and FFA measurement

TG, LDL/VLDL, HDL cholesterol and FFA concentration in serum and liver homogenate were measured using commercial kits according to manufacturer's protocol (Cayman Chemical).

Glucose and Pyruvate tolerance tests.

Pyruvate and glucose tolerance tests were performed on *ob/ob* animals at five days after GeRP treatment. Pyruvate (1 g/kg) and glucose (1 g/kg) were administered by intraperitoneal injection. Blood samples were withdrawn from the tail vein at the indicated time, and glycemia was determined using glucometers (Bayer-Breeze 2 and Abbott alphatrak).

Lipolysis assay

Epididymal fat pads were manually cut in small pieces and collagenase digested at 37°C for 20 minutes in Hank's buffered saline solution (HBSS) (Gibco, Life technologies) containing 2% bovine serum albumin (American Bioanalytical) and 2 mg/ml collagenase (Sigma-Aldrich). Samples were then filtered through 100 μm diameter pore nylon mesh and centrifuged. The adipocyte layer and the supernatant were collected and washed twice with PBS. Adipocytes were then incubated at 37°C in KRH buffer (12.6 mM NaCl, 0.14 M KCl, 1 M $CaCl_2$, 1.2 M $MgSO_4$, 1.2 M $KHPO_4$, 1 M Hepes, pH 7.2) in absence or presence of 10 μM isoproterenol (Sigma) for 2 hours. The medium was collected and assayed for glycerol content by using a commercial colorimetric assay kit from Sigma as per manufacturer's protocol.

aP2 secretion analysis

Adipocytes were isolated from untreated *ob/ob* mice and incubated for 1 hour in DMEM containing 10% fetal bovine serum and 1% penicillin/streptomycin. Adipocytes were then washed in PBS and incubated for 1 hour in the different conditioned media. Next, fresh media was added to adipocytes and aP2 was measured after 1 hour. aP2 levels in media and serum were measured by ELISA (Biovendor) according to the manufacturer's protocol.

Statistics

The statistical significance of the differences in the means of experimental groups was determined by Student's t-test or one-way or two-way ANOVA analysis and Bonferroni or Tukey's post-tests using GraphPad Prism 5.0a Software. The data are presented as the means ± s.e.m.

RESULTS and DISCUSSION

Lipid uptake by ATMs increases with obesity.

Most relevant literature describes ATMs as detrimental to whole body metabolism through secretion of inflammatory cytokines and other factors that may impair adipocyte function (18, 23, 30). However, recent work has indicated a beneficial role of ATMs, for example, in increasing adipose lipid storage (16). To determine the role of ATM lipid handling in systemic metabolism, we first measured the effect of obesity on formation of lipid-laden macrophages in the AT. Flow cytometry was performed on the stromal-vascular fraction (SVF) of six-week old obese *ob/ob* mice and wild-type (WT) lean controls, using antibodies against the macrophage markers, F4/80 and CD11b, and the lipid stain, bodipy (**Fig. 1**). We first confirmed that macrophage content was increased in epididymal AT (Visceral AT; VAT) of *ob/ob* compared to WT mice (Data not shown). Consistent with previous studies (25), the percentage of lipid-laden macrophages (defined as bodipy+/F4/80+/CD11b+) was significantly increased in the VAT of *ob/ob* compared to WT mice (**Fig. 1A-B**). To confirm the presence of foam cells in AT, fluorescence and

transmission electron microscopy (TEM) were performed on epididymal SVF of *ob/ob* mice (**Fig. 1C-D**). Figure 1C shows a representative macrophage (F4/80, red) containing lipid droplets (bodipy, green). Interestingly, lipid-laden ATMs were multi-nucleated as previously described (31). The TEM image presented shows a macrophage with characteristics described in previous studies (19, 30), with lipid droplets (arrows), confirming the presence of lipid-laden macrophages in the VAT of *ob/ob* mice (**Fig 1D**). Together these data indicate that lipid uptake by macrophages in the VAT is increased with obesity.

Consistent with an increased inflammatory state in the AT of obese mice, the expression of the inflammatory cytokines tumor necrosis factor alpha (TNF-α) and interleukin-1 beta (IL-1β) was significantly increased in *ob/ob* compared to WT AT (**Fig. 1E**). Surprisingly, while the expression of multiple genes involved in lipid uptake, synthesis and storage was decreased in the SVF of obese compared to WT animals, the expression of LPL was significantly higher in the SVF of obese compared to lean mice (**Fig. 1E**). Because the SVF contains multiple cell types, which could contribute to the variation in gene expression, we isolated ATMs using CD11b magnetic bead pull-down from WT and *ob/ob* AT. We then measured the expression of LPL as well as other genes involved in lipid metabolism, including fatty acid synthase (FASN), CD36, very-low-density lipoprotein receptor (VLDLr), peroxisome proliferator activated receptor γ (PPARγ), stearoyl-CoA desaturase-1 (SCD1) and fatty acid binding protein 4 (fabp4/aP2) (**Fig. 1F**). Similar to the SVF, only the expression of LPL was significantly increased in epididymal ATMs of *ob/ob* mice compared to their lean WT littermates **(Fig. 1F)**. This finding is consistent with data showing ATMs mostly accumulate lipids via activation of lipid uptake rather than *de novo* lipogenesis (25).

GeRP-mediated LPL silencing decreases lipid uptake by ATMs.

Primary peritoneal macrophages were used to screen for potent siRNAs against LPL, and two sequences were chosen **(Fig. 2A-B)**. Both siRNA sequences against the target gene significantly silenced the expression of LPL **(Fig. 2A)**. Furthermore, LPL protein levels

were significantly silenced by the targeting siRNAs compared to SCR siRNA or no treatment **(Fig. 2B)**. These data reveal that LPL can be depleted by LPL siRNA in primary macrophages *in vitro,* as detected either at the mRNA or protein levels.

To test the hypothesis that LPL is required for lipid uptake by macrophages in AT, LPL was selectively depleted in ATMs of obese mice by intraperitoneal (i.p.) injections with GeRPs loaded with scrambled (SCR) or LPL siRNA (see protocol outline in **Fig. 2C**). As previously described (2), silencing was specific to visceral phagocytes as no depletion of the target gene products was observed in livers of GeRP treated mice **(Fig. 2D)**. Other studies we have performed showed no gene silencing with this technique in macrophages present in other tissues of the obese mice, including lung, pancreas, spleen and muscle (2). LPL protein levels in SVF isolated from epididymal AT of mice treated with LPL-GeRPs were also significantly reduced compared to mice treated with SCR-GeRPs (**Fig. 2E**). Importantly, flow cytometry showed that silencing LPL in ATMs significantly decreased lipid accumulation in VAT macrophage (**Fig. 2F-G**), while it had no effect on total macrophage content in VAT (Data not shown). Careful analysis of epididymal AT sections by TEM showed lipid droplets in macrophages containing GeRPs within AT. Treatment with LPL-GeRPs reduced the presence of these lipid droplets in ATM (**Fig. 2H**). These results suggested that ATM LPL contributes to obesity-induced lipid uptake by macrophages in VAT.

LPL silencing in ATMs increases serum FFA levels.

Although lipid uptake by ATMs has been suggested to contribute to lipid storage in AT (4, 16), LPL deficiency in macrophages throughout the body did not regulate adiposity in mice fed a HFD (28). Similarly, we found that body weight gain, epididymal fad pad weight, adipocyte number and size were unchanged following LPL silencing specific to epididymal ATMs over this relatively short period (Data not shown). Treatment of *ob/ob* mice with LPL-GeRPs also had no impact on serum TG levels, LDL/VLDL- and HDL-cholesterol **(Fig. 3A-B)**, consistent with a recent study showing that LPL depletion in the myeloid lineage has no effect on circulating TG and cholesterol levels (28). Therefore

steady state circulating TG levels could be maintained in mice treated with LPL-GeRPs compared to SCR-GeRPs by the normal expression of LPL in other tissues.

Although LPL silencing had no impact on serum TG and cholesterol levels, serum FFA levels were significantly increased following ATM LPL silencing (**Fig. 3C**). One study suggested that ATMs can buffer local increases in lipid and suppress local adipocyte lipolysis, decreasing lipid levels in the circulation (16). In an effort to test whether LPL silencing in ATMs increased serum FFA levels through regulation of lipid release by adipocytes, we found that LPL depletion in ATMs had no effect on the expression of hormone-sensitive lipase (HSL) and adipose triglyceride lipase (ATGL), involved in lipolysis (**Fig. 3D**). In addition, lipolysis under basal conditions or following beta-adrenergic stimulation by isoproterenol remained unchanged in isolated adipocytes derived from mice treated with LPL-GeRPs or SCR-GeRPs (**Fig. 3E**). Consistently, LPL-GeRP treatment had no effect on serum glycerol levels in mice fasted overnight (data not shown). These results suggested that the increased circulating FFA levels observed in mice treated with LPL-GeRPs could be due to a decreased ability of ATMs to store excess lipids released by adipocytes in the obese state rather than a direct regulation of lipolysis by macrophages.

In testing this idea, we found LPL silencing in ATMs not only decreased LPL mRNA, but also caused an overall trend towards decreasing the expression of genes involved in lipid metabolism in SVF (**Fig. 3F**). LPL silencing in ATMs also resulted in a significant decrease of CD36 and DGAT2 expression when measured in SVF cells isolated by fluorescence activated cell sorting (FACS) on the basis of their FITC-GeRP signal. This was consistent with a decreased FFA uptake and esterification by ATMs following LPL silencing (**Fig. 3G**). To confirm this hypothesis, we measured the percentage of foam cells in AT following fasting-induced lipolysis (**Fig. 3H**). Consistent with the idea that ATMs take up FFA released by adipocytes in fasting condition (16), in obese mice treated with PBS, fasting increased the percentage of bodipy^{+} ATMs (**Fig. 3H**). Furthermore, flow cytometry analysis showed that the increase bodipy^{+} ATMs under fasting condition was blocked following LPL silencing in ATMs (**Fig. 3H**). Taken together, these results suggest that silencing LPL unexpectedly decreases the capacity of

ATMs to take up the excess FFA released by adipocytes. A potential mechanism for this surprising effect may relate to studies suggesting that hydrolysis of TG by LPL releases ligands for PPARα/δ transcription factors known to drive the expression of lipogenic genes including DGAT2 and CD36 that are decreased by ATM LPL silencing (9, 32). However, LPL silencing decreased the expression of CD36 and DGAT2, while the expression of other PPAR target genes remained unchanged. Although additional work would be needed to unravel the mechanism whereby LPL silencing secondarily decreases CD36 and DGAT2 gene expression, previous studies (8, 22) as well as our work suggest that different transcription factors, co-activators or repressors may be involved in the transcriptional regulation of lipogenic genes in macrophages deficient in LPL.

Silencing LPL in visceral ATMs exacerbates glucose intolerance in *ob/ob* mice.

Increased serum FFA levels have been shown to positively regulate glucose production by liver (6, 10, 12). Although hepatic steatosis, as observed in H&E liver sections and liver TG content, was unchanged following LPL silencing (**Fig. 4A-B**), the expression of two gluconeogenic enzymes, phosphoenolpyruvate carboxykinase (PEPCK) and glucose-6-phosphatase (G6Pase), was significantly increased in livers from ob/ob mice treated with LPL- compared to SCR-GeRPs (**Fig. 4C**). To further assess hepatic glucose production, mice were challenged with the gluconeogenic precursor, pyruvate (**Fig. 4D**). Silencing LPL in visceral ATMs exacerbated pyruvate intolerance in mice treated with LPL- compared to SCR-GeRPs (**Fig. 4D**). Given that increased hepatic glucose output often results in exacerbated systemic glucose tolerance, we performed glucose tolerance tests (GTT) in *ob/ob* mice treated with LPL-GeRPs or SCR-GeRPs **(Fig. 4E)**. Mice treated with LPL-GeRPs were significantly less glucose tolerant compared to mice treated with SCR-GeRPs **(Fig. 4E)**. This effect on glucose tolerance occurred independently of an effect on insulin tolerance, fasting glucose or insulin levels, or islet morphology (data not shown).

Since LPL silencing resulted in a significant decrease in CD36 expression in ATMs, we also performed GTT in mice treated with SCR- or CD36-GeRPs. Similar to LPL silencing, CD36 knockdown in ATMs lead to a further impairment of glucose tolerance

in *ob/ob* mice (**Fig. 4F**). However, CD36 deficiency in hematopoietic cells obtained with bone marrow transplantation was shown to decrease the accumulation of immune cells within adipose tissue in obesity, with a concomitant improvement in insulin action (20). This discrepancy could be explained by the use of bone-marrow transplantation in this previous study, which affects all immune cells rather than phagocytes specifically. Indeed, CD36 has been shown to play opposite roles in the regulation of insulin sensitivity depending on the tissue in which it functions (13). Interestingly, treatment of lean healthy mice with LPL-GeRPs had no significant effect on glucose tolerance or circulating FFA (**Fig. 4G-H)**. This confirmed the ability of AT in lean healthy mice to appropriately store lipids and the minimal role that ATMs play in this process in lean mice. However, ATMs may contribute to lipid storage in the AT of obese mice thus preventing glucose intolerance induced by increased circulating FFA.

Silencing LPL in visceral ATMs increases fatty aP2 production by adipocytes in *ob/ob* mice.

To further investigate the mechanism whereby LPL silencing in ATMs exacerbates glucose intolerance in obese mice, we measured the expression of lipogenic and inflammatory genes in the AT of mice treated with LPL-GeRPs compared to SCR-GeRPs (**Fig. 5A**). Interestingly, while the expression of several lipogenic and inflammation-related genes remained unchanged, the expression of aP2 was significantly increased in the AT of mice treated with LPL-GeRPs (**Fig. 5A**). Moreover, RT-PCR analysis revealed that aP2 expression was significantly increased in isolated adipocytes recovered from VAT of mice treated with LPL-GeRPs compared to SCR-GeRPs (**Fig. 5B**). Importantly, aP2 levels in the serum were also significantly increased in mice treated with LPL-GeRPs compared to SCR-GeRPs (**Fig. 5C**). Interestingly, a recent study showed that aP2 could be secreted by adipocytes (6). To test this hypothesis, primary adipocytes were treated with media containing 10% serum or conditioned media of SVF isolated from *ob/ob* mice treated with SCR- or LPL-GeRPs (**Fig. 5D**). After 1-hour incubation media was removed and fresh media was added to avoid measurement of aP2 present in conditioned media. While media of SVF had no effect on aP2 protein levels, we found that treatment of adipocytes with serum from mice treated with LPL-GeRPs increased aP2 levels

compared to serum of mice treated with SCR-GeRPs (**Fig. 5D**). These results confirmed that silencing LPL in ATMs induces aP2 secretion from adipocytes and showed that this regulation occurs through an endocrine rather than a paracrine mechanism. Interestingly, although secretion of aP2 from adipocytes has been shown to be regulated by lipolysis-related signals (6), in our model aP2 production by adipocytes occurred independently of an effect on lipolysis (**Fig. 3E**).

Because treatment of mice with recombinant aP2 has been shown to increase hepatic glucose production, while aP2 neutralization reduced it (6), silencing LPL in ATMs may exacerbate glucose intolerance and hepatic glucose production not only by increasing circulating FFA but also by inducing aP2 secretion. Taken together these results show that silencing LPL in ATMs exacerbates glucose intolerance and hepatic glucose production (See model in **Fig. 6**). This impairment in glucose homeostasis is accompanied by an increase in serum FFA and aP2 levels in obese mice. Additional work will be needed to test whether there is a causal relationship between the increases in serum FFA and aP2 and glucose intolerance in obese mice following LPL silencing in ATMs.

ACKNOWLEDGEMENTS

We thank members of our laboratory group for excellent discussion of the data in this paper. We also appreciate the help of the Flow Cytometry and the Confocal Microscopy Core Facilities, and we thank Gregory Hendricks and Lara Strittmatter at the University of Massachusetts Medical School for the electron micrographs, supported by a grant from the National Center For Research Resources (S10RR027897).

GRANTS

These studies were supported by grants to M.P.C. from the National Institutes of Health (DK085753, AI046629, DK030898) and the International Research Alliance of the Novo Nordisk Foundation Center for Metabolic Research. We also acknowledge the invaluable

help of the morphology Core Facility at the University of Massachusetts Diabetes and Endocrinology Research Center, also funded by the National Institutes of Health (DK325220). J.L.C. is supported by the National Institute of Diabetes and Digestive and Kidney Diseases of the National Institutes of Health under NRSA postdoctoral fellowship F32DK098879. J.C.Y. is supported by a predoctoral Ruth L. Kirschstein National Research Service Award from the NIH (DK096948-02).

DISCLOSURES

The authors declare no conflict of interest.

FIGURE LEGENDS

Figure 1. Formation of lipid-laden macrophages in epididymal AT of obese mice. SVF from epididymal AT (Visceral AT; VAT) of WT and *ob*/*ob* mice was isolated and analyzed by flow cytometry. (**A**) Representative flow cytometry dot plots and mean fluorescence intensity (MFI) of ATMs stained with bodipy. (**B**) Percentage of macrophages stained with bodipy. n=10. (**C**) Microscopy of SVF isolated from *ob*/*ob* VAT stained with antibodies against F4/80 (red) and bodipy (green); 20x (scale bar = 50 μm). (**D**) TEM of whole VAT of *ob*/*ob* mice; A, adipocyte; M, macrophage; arrows, lipid droplet. Scale bar = 2 μm. (**E**) Gene expression measured by RT-PCR in SVF isolated from VAT of WT and *ob*/*ob* mice. n=5. Results are the mean fold change (F.C.) ± s.e.m. (**F**) Gene expression measured by RT-PCR in macrophages isolated using CD11b antibody bound to magnetic beads. n=5. All graphs are expressed as mean ± s.e.m. Statistical significance was determined by Student's t-test. ***$p<0.001$; **$p<0.01$; *$p<0.05$.

Figure 2. GeRP-mediated ATM LPL silencing decreases formation of lipid-laden macrophages in visceral AT of obese mice. Peritoneal macrophages **(**1x 10^6) were treated with particles made with a mixture of 160 pmoles siRNA and 3 nmoles EP. Forty-eight hours after the treatment, mRNA levels were measured by (**A**) RT-PCR and protein by (**B**) western-blot. (**C**) Outline of the GeRP treatment given to mice. Briefly, mice were injected for five consecutive days with 5.6 mg of GeRPs/kg of body weight loaded with 262 μg of siRNA/kg of body weight and 2.1 mg of EP/kg of body weight. On day 6, tissues were isolated. (**D**) mRNA expression of LPL in VAT and liver from mice treated with SCR- or LPL-GeRPs. n=14-15. **(E)** Representative LPL western-blot and densitometry using epididymal SVF lysates from mice treated with SCR- or LPL -GeRPs. Actin was used as a loading control. Statistical significance was determined by Student's t-test. **p < 0.01; *p < 0.05. (**F**) Representative flow cytometry dot plots and MFI of ATMs stained with bodipy. (**G**) Percentage of macrophages expressing bodipy. n=10.All graphs are expressed as mean ± s.e.m. Statistical significance was determined by Student's t-test. ***p<0.001; **p<0.01; *p<0.05. (**H**) TEM of whole VAT from *ob*/*ob* mice treated with SCR- or LPL-GeRPs; A, adipocyte; arrows, GeRPs. Scale bar = 5 μm.

Figure 3. LPL silencing in ATMs increases plasma FFA. (A) Serum triglyceride and **(B)** LDL/VLDL and HDL cholesterol in mice treated with SCR- or LPL-GeRPs. n=10. **(C)** Serum FFA levels. n=14-15. **(D)** ATGL and HSL expression in adipocytes isolated from *ob*/*ob* mice treated with SCR- or LPL-GeRPs. n=14-15. **(E)** Glycerol levels in media of isolated adipocytes in untreated (UNT) or treated with 10 μM isoproterenol (ISO) for 2 hours. n=5. Gene expression measured by RT-PCR in **(F)** SVF (n=14-15) and **(G)** ATMs containing GeRPs sorted by FACS (n=5). **(H)** Representative Dot-plot and percentage of ATMs expressing bodipy in fed and fasted states in VAT. n=10. All graphs are expressed as mean ± s.e.m. Statistical significance was determined by Student's t-test. ***p<0.001; *p<0.05; n/s, not significant.

Figure 4. LPL silencing in ATMs exacerbates glucose intolerance in *ob/ob* mice. (**A**) H&E liver sections of mice treated with SCR- or LPL GeRPs. 20x magnification images.

Scale bar = 5 µm. (**B**) Liver TG content. n=10. (**C**) PEPCK and G6Pase expression in liver of *ob*/*ob* mice treated with SCR- or LPL-GeRPs. n=10. (**D**) Pyruvate tolerance test, and area under the curve (AUC). n=10. (**E**) Glucose tolerance tests and AUC, n=14-15, performed on mice that were fasted for 18 hours. (**F**) Glucose tolerance tests performed on *ob/ob* mice treated with SCR- or CD36-GeRPs, n=5. (**G**) Glucose tolerance tests performed on 8 week-old C57BL6 lean mice treated with SCR- or LPL-GeRPs. n=5. (**H**) Serum FFA levels in lean mice treated with SCR- or LPL-GeRPs. n=5. Results are mean ± s.e.m. Statistical significance was determined by T-test or ANOVA and Tukey's post test. ***$p<0.001$; *$p < 0.05$.

Figure 5. LPL silencing in ATMs increases aP2 production by adipocytes. (**A**) Gene expression measured by RT-PCR in (**A**) VAT and (**B**) adipocytes isolated from of *ob*/*ob* mice treated with SCR- or LPL-GeRPs. n=14-15. **(C)** Serum aP2 levels. n=14-15. (**D**) aP2 protein levels in media of intact adipocytes measured by ELISA. Adipocytes were treated with media containing serum or conditioned media from SVF. n=4. Results are mean ± s.e.m. Statistical significance was determined by T-test or ANOVA and Tukey's post test. *$p < 0.05$.

Figure 6. Hypothetical model for how LPL produced by ATMs can regulate whole body glucose metabolism. LPL silencing in ATMs secondarily decreases the expression of CD36 and DGAT2 by mechanisms not understood. This results in a reduced lipid uptake (via CD36) and esterification (via DGAT2) by ATMs and a concomitant increase in circulating FFA. In parallel, silencing LPL in ATMs is accompanied by an increase in aP2 expression and secretion by adipocytes. The increases in circulating aP2 and FFA may enhance hepatic gluconeogenesis, thus contributing to the impairment of glucose tolerance observed in *ob/ob* mice following LPL silencing in ATMs. Short vertical arrows indicate the effects (arrow up, increase; arrow down, decrease) on specific components or pathways in response to silencing LPL in ATMs.

REFERENCES

1. **Adeyo O, Goulbourne CN, Bensadoun A, Beigneux AP, Fong LG, and Young**

SG. Glycosylphosphatidylinositol-anchored high-density lipoprotein-binding protein 1 and the intravascular processing of triglyceride-rich lipoproteins. *J Intern Med* 272: 528-540, 2012.

2. **Aouadi M, Tencerova M, Vangala P, Yawe JC, Nicoloro SM, Amano SU, Cohen JL, and Czech MP**. Gene silencing in adipose tissue macrophages regulates whole body metabolism in obese mice. *Proc Natl Acad Sci U S A* 2013.

3. **Aouadi M, Tesz GJ, Nicoloro SM, Wang M, Chouinard M, Soto E, Ostroff GR, and Czech MP**. Orally delivered siRNA targeting macrophage Map4k4 suppresses systemic inflammation. *Nature* 458: 1180-1184, 2009.

4. **Asterholm IW, McDonald J, Blanchard PG, Sinha M, Xiao Q, Mistry J, Rutkowski JM, Deshaies Y, Brekken RA, and Scherer PE**. Lack of "immunological fitness" during fasting in metabolically challenged animals. *J Lipid Res* 53: 1254-1267, 2012.

5. **Babaev VR, Patel MB, Semenkovich CF, Fazio S, and Linton MF**. Macrophage lipoprotein lipase promotes foam cell formation and atherosclerosis in low density lipoprotein receptor-deficient mice. *J Biol Chem* 275: 26293-26299, 2000.

6. **Cao H, Sekiya M, Ertunc ME, Burak MF, Mayers JR, White A, Inouye K, Rickey LM, Ercal BC, Furuhashi M, Tuncman G, and Hotamisligil GS**. Adipocyte lipid chaperone AP2 is a secreted adipokine regulating hepatic glucose production. *Cell Metab* 17: 768-778, 2013.

7. **Cao Y**. Angiogenesis modulates adipogenesis and obesity. *J Clin Invest* 117: 2362-2368, 2007.

8. **Chawla A, Barak Y, Nagy L, Liao D, Tontonoz P, and Evans RM**. PPAR-gamma dependent and independent effects on macrophage-gene expression in lipid metabolism and inflammation. *Nat Med* 7: 48-52, 2001.

9. **Chawla A, Lee CH, Barak Y, He W, Rosenfeld J, Liao D, Han J, Kang H, and Evans RM**. PPARdelta is a very low-density lipoprotein sensor in macrophages. *Proc Natl Acad Sci U S A* 100: 1268-1273, 2003.

10. **Chen X, Iqbal N, and Boden G**. The effects of free fatty acids on gluconeogenesis and glycogenolysis in normal subjects. *J Clin Invest* 103: 365-372, 1999.

11. **Christiaens V, and Lijnen HR**. Angiogenesis and development of adipose tissue. *Mol Cell Endocrinol* 318: 2-9, 2010.

12. **Donnelly KL, Smith CI, Schwarzenberg SJ, Jessurun J, Boldt MD, and Parks EJ**. Sources of fatty acids stored in liver and secreted via lipoproteins in patients with nonalcoholic fatty liver disease. *J Clin Invest* 115: 1343-1351, 2005.

13. **Goudriaan JR, Dahlmans VE, Teusink B, Ouwens DM, Febbraio M, Maassen JA, Romijn JA, Havekes LM, and Voshol PJ**. CD36 deficiency increases insulin sensitivity in muscle, but induces insulin resistance in the liver in mice. *J Lipid Res* 44: 2270-2277, 2003.

14. **Guilherme A, Virbasius JV, Puri V, and Czech MP**. Adipocyte dysfunctions linking obesity to insulin resistance and type 2 diabetes. *Nat Rev Mol Cell Biol* 9: 367-377, 2008.

15. **Halberg N, Khan T, Trujillo ME, Wernstedt-Asterholm I, Attie AD, Sherwani S, Wang ZV, Landskroner-Eiger S, Dineen S, Magalang UJ, Brekken RA, and Scherer PE**. Hypoxia-inducible factor 1alpha induces fibrosis and insulin resistance in white adipose tissue. *Mol Cell Biol* 29: 4467-4483, 2009.

16. **Kosteli A, Sugaru E, Haemmerle G, Martin JF, Lei J, Zechner R, and Ferrante AW, Jr.** Weight loss and lipolysis promote a dynamic immune response in murine adipose tissue. *J Clin Invest* 120: 3466-3479, 2010.

17. **Kusminski CM, Shetty S, Orci L, Unger RH, and Scherer PE**. Diabetes and apoptosis: lipotoxicity. *Apoptosis* 14: 1484-1495, 2009.

18. **Lumeng CN, and Saltiel AR**. Inflammatory links between obesity and metabolic disease. *J Clin Invest* 121: 2111-2117, 2011.

19. **Murano I, Barbatelli G, Parisani V, Latini C, Muzzonigro G, Castellucci M, and Cinti S**. Dead adipocytes, detected as crown-like structures, are prevalent in visceral fat depots of genetically obese mice. *J Lipid Res* 49: 1562-1568, 2008.

20. **Nicholls HT, Kowalski G, Kennedy DJ, Risis S, Zaffino LA, Watson N, Kanellakis P, Watt MJ, Bobik A, Bonen A, Febbraio M, Lancaster GI, and Febbraio MA**. Hematopoietic cell-restricted deletion of CD36 reduces high-fat diet-induced macrophage infiltration and improves insulin signaling in adipose tissue. *Diabetes* 60: 1100-1110, 2011.

21. **Obunike JC, Lutz EP, Li Z, Paka L, Katopodis T, Strickland DK, Kozarsky KF, Pillarisetti S, and Goldberg IJ**. Transcytosis of lipoprotein lipase across cultured endothelial cells requires both heparan sulfate proteoglycans and the very low density lipoprotein receptor. *J Biol Chem* 276: 8934-8941, 2001.

22. **Olagnier D, Lavergne RA, Meunier E, Lefevre L, Dardenne C, Aubouy A, Benoit-Vical F, Ryffel B, Coste A, Berry A, and Pipy B**. Nrf2, a PPARgamma alternative pathway to promote CD36 expression on inflammatory macrophages: implication for malaria. *PLoS Pathog* 7: e1002254, 2011.

23. **Olefsky JM, and Glass CK**. Macrophages, inflammation, and insulin resistance. *Annu Rev Physiol* 72: 219-246, 2010.

24. **Pang C, Gao Z, Yin J, Zhang J, Jia W, and Ye J**. Macrophage infiltration into adipose tissue may promote angiogenesis for adipose tissue remodeling in obesity. *Am J Physiol Endocrinol Metab* 295: E313-322, 2008.

25. **Prieur X, Mok CY, Velagapudi VR, Nunez V, Fuentes L, Montaner D, Ishikawa K, Camacho A, Barbarroja N, O'Rahilly S, Sethi JK, Dopazo J, Oresic M, Ricote M, and Vidal-Puig A**. Differential lipid partitioning between adipocytes and tissue macrophages modulates macrophage lipotoxicity and M2/M1 polarization in obese mice. *Diabetes* 60: 797-809, 2011.

26. **Samuel VT, Petersen KF, and Shulman GI**. Lipid-induced insulin resistance: unravelling the mechanism. *Lancet* 375: 2267-2277, 2010.

27. **Sun K, Kusminski CM, and Scherer PE**. Adipose tissue remodeling and obesity. *J Clin Invest* 121: 2094-2101, 2011.

28. **Takahashi M, Yagyu H, Tazoe F, Nagashima S, Ohshiro T, Okada K, Osuga J, Goldberg IJ, and Ishibashi S**. Macrophage lipoprotein lipase modulates the development of atherosclerosis but not adiposity. *J Lipid Res* 54: 1124-1134, 2013.

29. **Tesz GJ, Aouadi M, Prot M, Nicoloro SM, Boutet E, Amano SU, Goller A, Wang M, Guo CA, Salomon WE, Virbasius JV, Baum RA, O'Connor MJ, Jr., Soto E, Ostroff GR, and Czech MP**. Glucan particles for selective delivery of siRNA to phagocytic cells in mice. *Biochem J* 436: 351-362, 2011.

30. **Weisberg SP, McCann D, Desai M, Rosenbaum M, Leibel RL, and Ferrante AW, Jr.** Obesity is associated with macrophage accumulation in adipose tissue. *J Clin*

Invest 112: 1796-1808, 2003.

31. **Xu X, Grijalva A, Skowronski A, van Eijk M, Serlie MJ, and Ferrante AW, Jr.** Obesity activates a program of lysosomal-dependent lipid metabolism in adipose tissue macrophages independently of classic activation. *Cell Metab* 18: 816-830, 2013.

32. **Ziouzenkova O, Perrey S, Asatryan L, Hwang J, MacNaul KL, Moller DE, Rader DJ, Sevanian A, Zechner R, Hoefler G, and Plutzky J**. Lipolysis of triglyceride-rich lipoproteins generates PPAR ligands: evidence for an antiinflammatory role for lipoprotein lipase. *Proc Natl Acad Sci U S A* 100: 2730-2735, 2003.

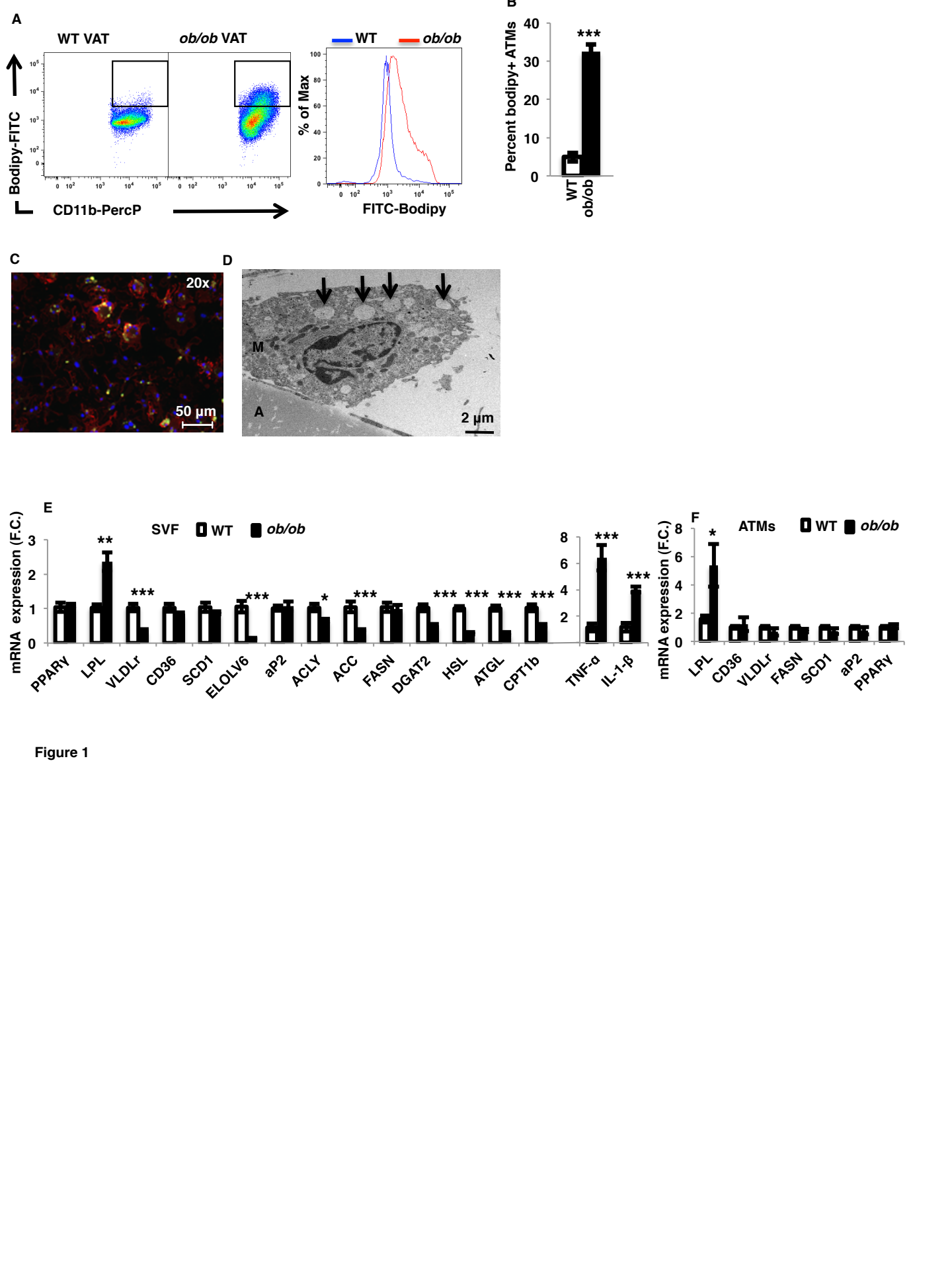
A
WT VAT
ob/ob VAT
Bodipy-FITC
CD11b-PercP
WT
ob/ob
% of Max
FITC-Bodipy
B
Percent bodipy+ ATMs
***
WT
ob/ob
C
20x
50 µm
D
M
A
2 µm
E
SVF
WT
ob/ob
mRNA expression (F.C.)
PPARγ
LPL
VLDLr
CD36
SCD1
ELOLV6
aP2
ACLY
ACC
FASN
DGAT2
HSL
ATGL
CPT1b
TNF-α
IL-1-β
F
ATMs
WT
ob/ob
mRNA expression (F.C.)
LPL
CD36
VLDLr
FASN
SCD1
aP2
PPARγ

Figure 1

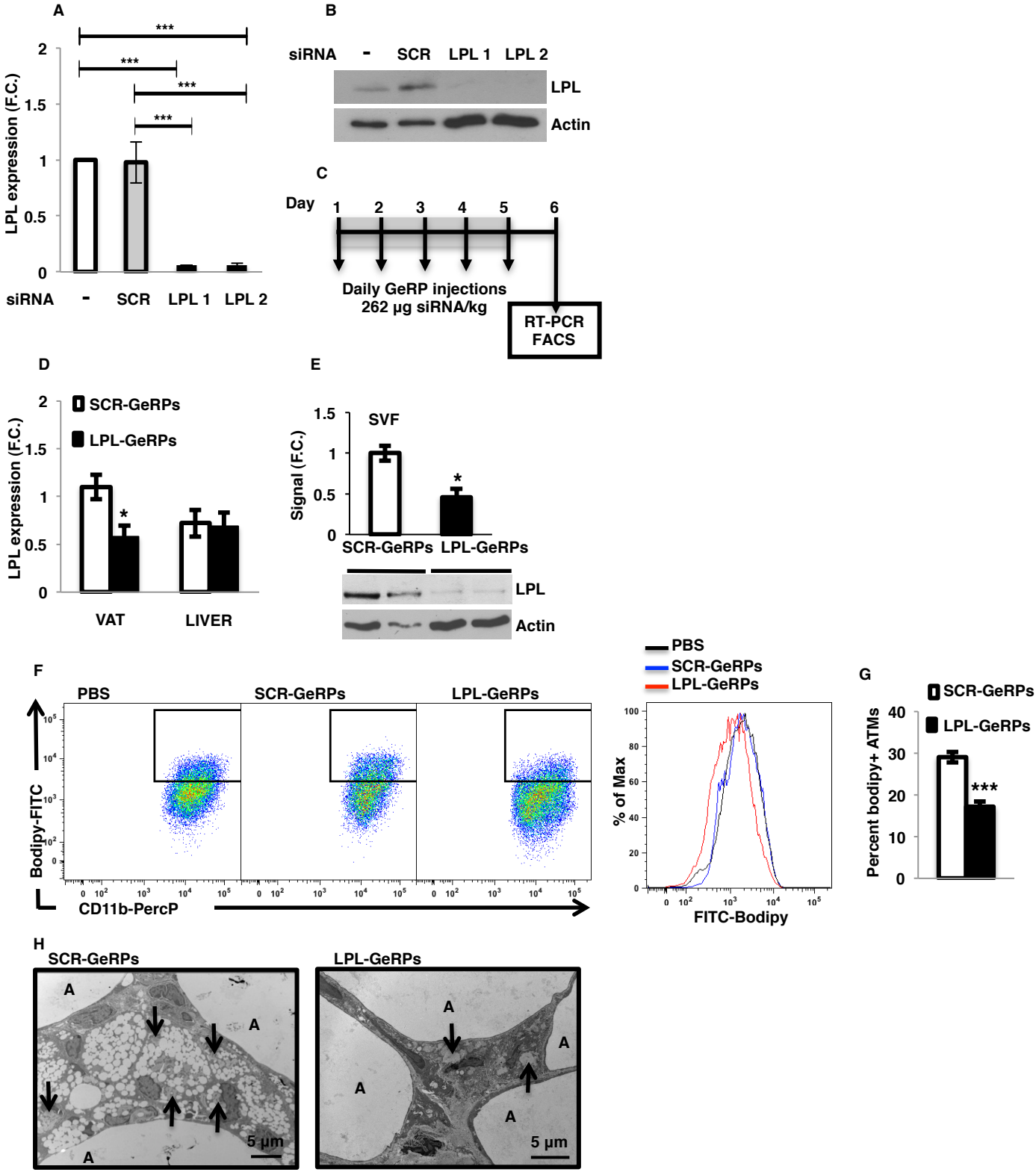
A
B
C
D
E
F
G
H
LPL expression (F.C.)
siRNA
SCR
LPL 1
LPL 2
LPL
Actin
Day
Daily GeRP injections
262 µg siRNA/kg
RT-PCR
FACS
SCR-GeRPs
LPL-GeRPs
VAT
LIVER
SVF
Signal (F.C.)
PBS
Bodipy-FITC
CD11b-PercP
% of Max
FITC-Bodipy
Percent bodipy+ ATMs
5 µm

Figure 2

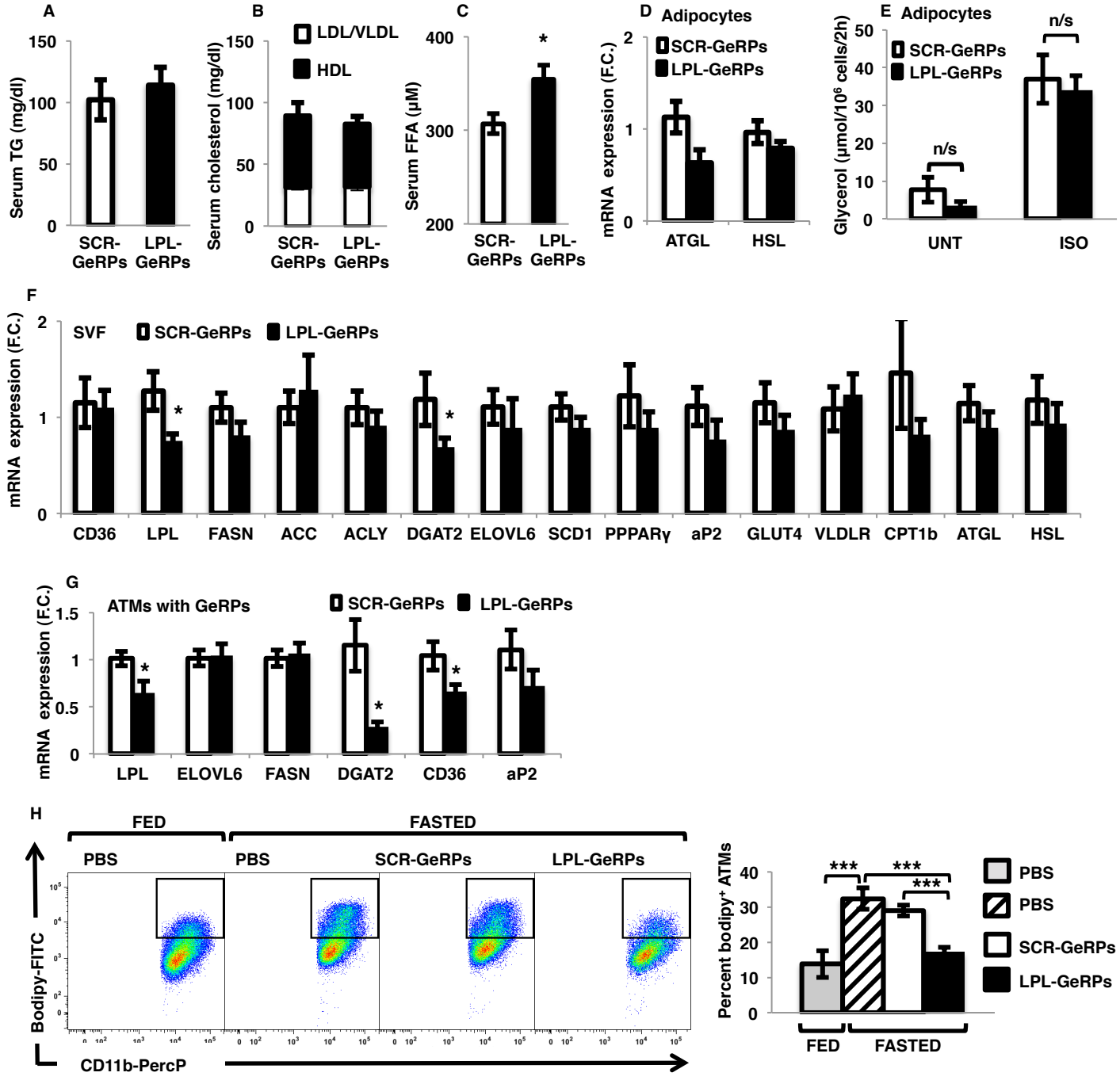
A
Serum TG (mg/dl)
150
100
50
0
SCR-GeRPs
LPL-GeRPs
B
Serum cholesterol (mg/dl)
LDL/VLDL
HDL
C
Serum FFA (μM)
400
300
200
*
D Adipocytes
mRNA expression (F.C.)
SCR-GeRPs
LPL-GeRPs
ATGL
HSL
E Adipocytes
Glycerol (μmol/10^6 cells/2h)
n/s
UNT
ISO
F
SVF
mRNA expression (F.C.)
CD36
LPL
FASN
ACC
ACLY
DGAT2
ELOVL6
SCD1
PPPARγ
aP2
GLUT4
VLDLR
CPT1b
ATGL
HSL
G
ATMs with GeRPs
mRNA expression (F.C.)
LPL
ELOVL6
FASN
DGAT2
CD36
aP2
H
FED
FASTED
PBS
PBS
SCR-GeRPs
LPL-GeRPs
Bodipy-FITC
CD11b-PercP
Percent bodipy+ ATMs
***
PBS
PBS
SCR-GeRPs
LPL-GeRPs

Figure 3

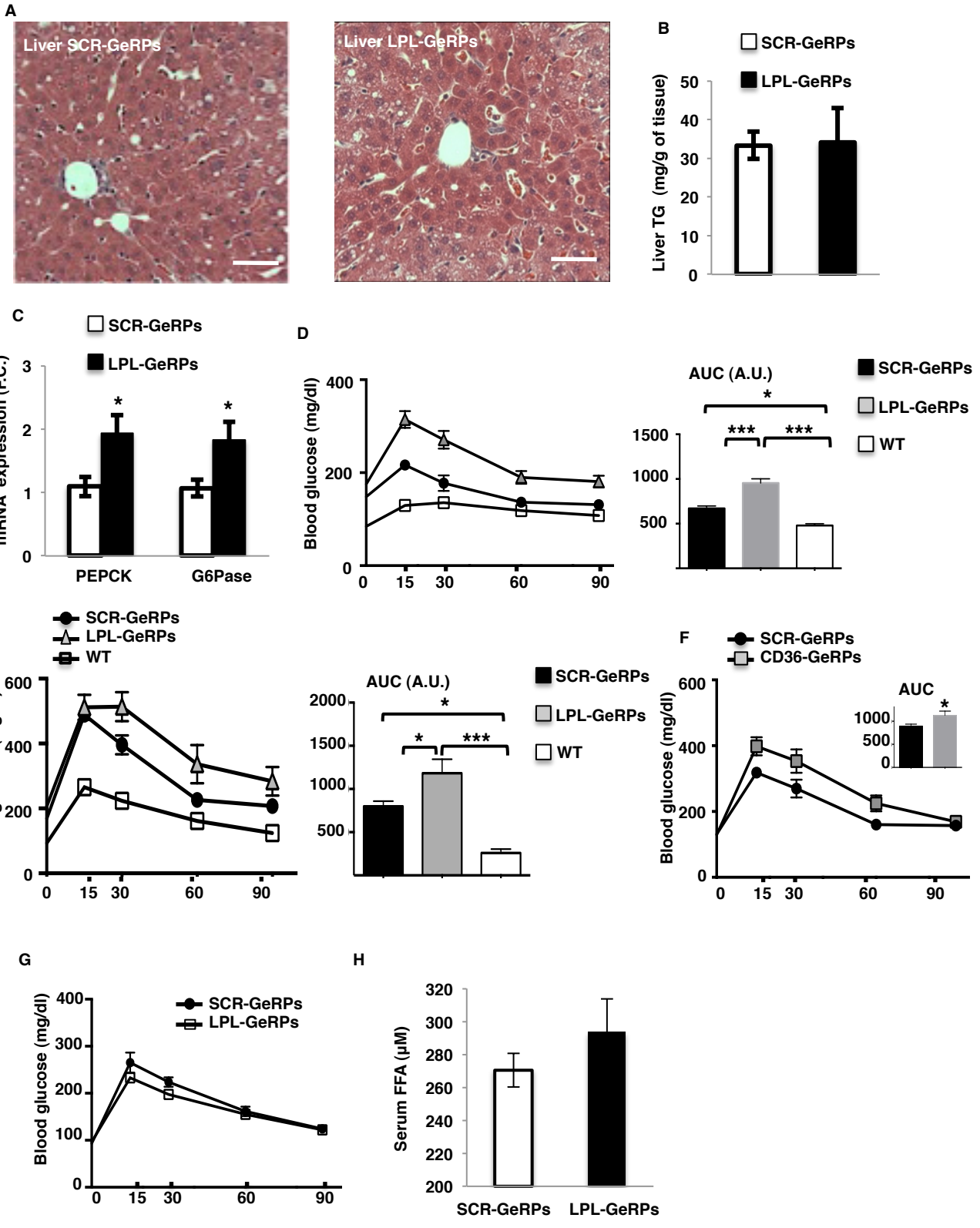
A
Liver SCR-GeRPs
Liver LPL-GeRPs
B
SCR-GeRPs
LPL-GeRPs
Liver TG (mg/g of tissue)
50
40
30
20
10
0
C
SCR-GeRPs
LPL-GeRPs
mRNA expression (F.C.)
3
2
1
0
*
*
PEPCK
G6Pase
D
Blood glucose (mg/dl)
400
200
0
0
15
30
60
90
AUC (A.U.)
*
***
***
1500
1000
500
SCR-GeRPs
LPL-GeRPs
WT
E
SCR-GeRPs
LPL-GeRPs
WT
Blood glucose (mg/dl)
600
400
200
0
0
15
30
60
90
AUC (A.U.)
2000
1500
1000
500
*
*
***
SCR-GeRPs
LPL-GeRPs
WT
F
SCR-GeRPs
CD36-GeRPs
Blood glucose (mg/dl)
600
400
200
0
0
15
30
60
90
AUC
1000
500
0
*
G
SCR-GeRPs
LPL-GeRPs
Blood glucose (mg/dl)
400
300
200
100
0
0
15
30
60
90
H
Serum FFA (μM)
320
300
280
260
240
220
200
SCR-GeRPs
LPL-GeRPs

Figure 4

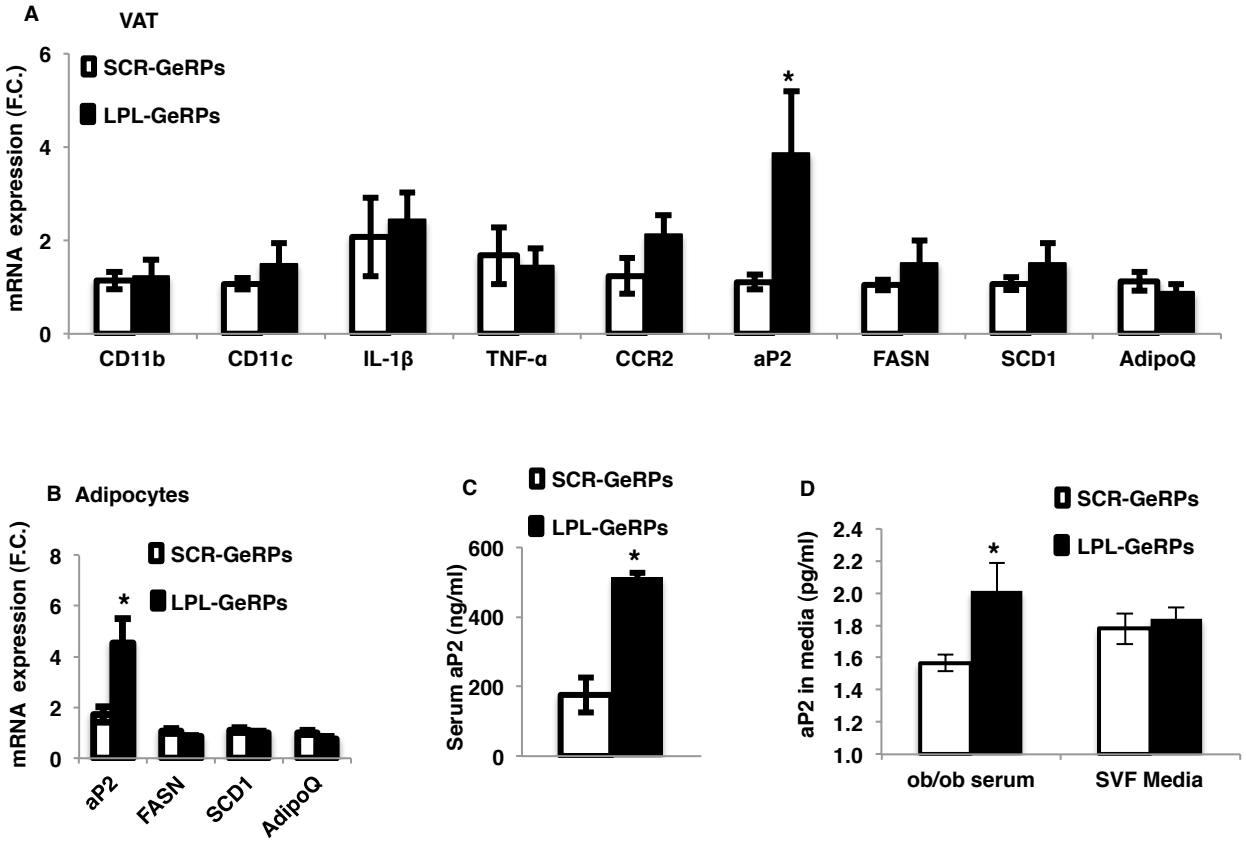
A
VAT
SCR-GeRPs
LPL-GeRPs
mRNA expression (F.C.)
0
2
4
6
*
CD11b
CD11c
IL-1β
TNF-α
CCR2
aP2
FASN
SCD1
AdipoQ
B Adipocytes
SCR-GeRPs
LPL-GeRPs
mRNA expression (F.C.)
0
2
4
6
8
*
aP2
FASN
SCD1
AdipoQ
C
SCR-GeRPs
LPL-GeRPs
Serum aP2 (ng/ml)
0
200
400
600
*
D
SCR-GeRPs
LPL-GeRPs
aP2 in media (pg/ml)
1.0
1.2
1.4
1.6
1.8
2.0
2.2
2.4
*
ob/ob serum
SVF Media

Figure 5

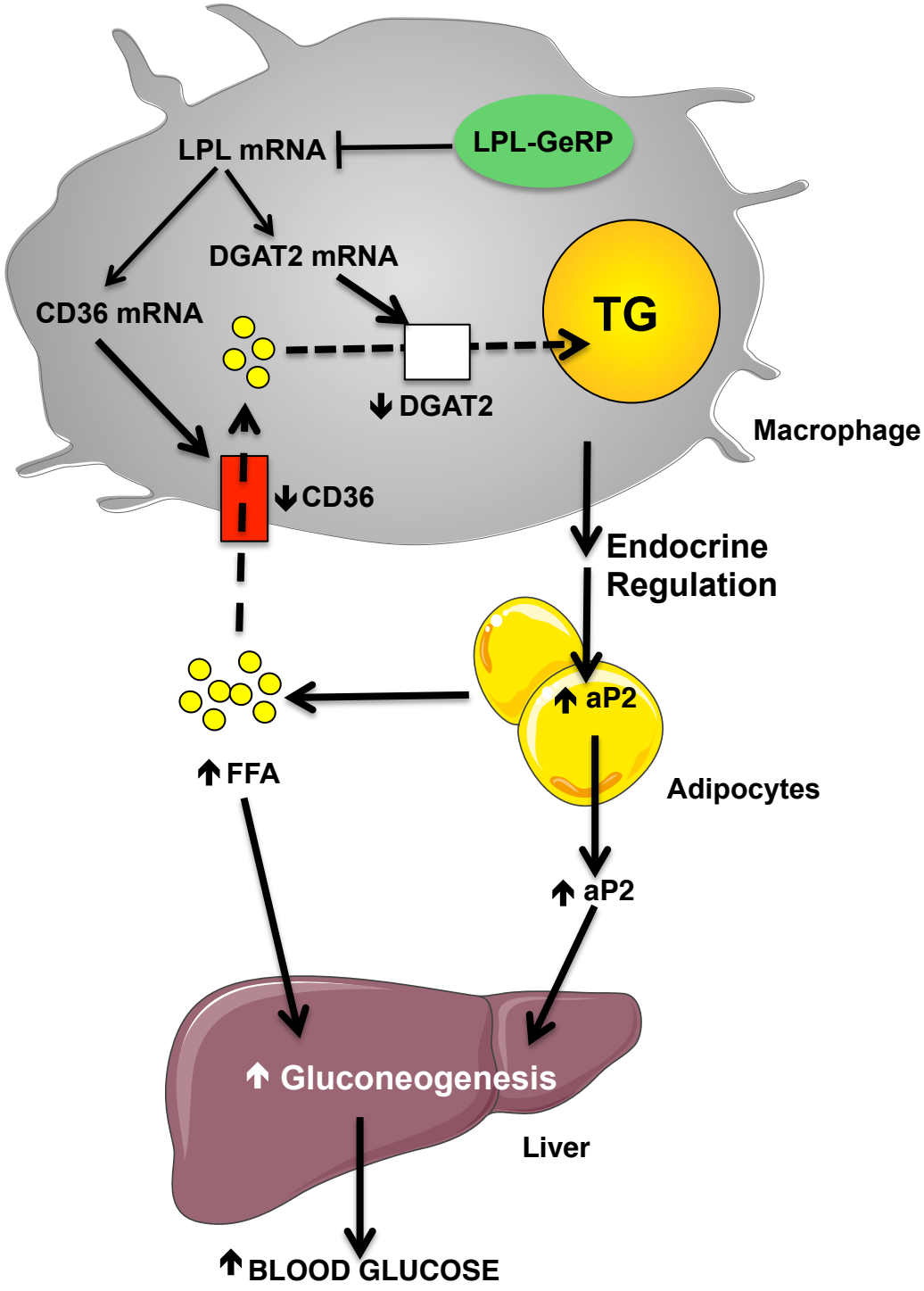
LPL mRNA
LPL-GeRP
DGAT2 mRNA
CD36 mRNA
TG
DGAT2
Macrophage
CD36
Endocrine
Regulation
aP2
FFA
Adipocytes
aP2
Gluconeogenesis
Liver
BLOOD GLUCOSE